Effect of growth time on structural and surface properties of TiO2 nanostructures deposited by single-step hydrothermal method

A. Lahmar, M. Jouiad, M. El Marssi, H. Mezzourh, S. Ben Moumen, M. Amjoud, D. Mezzane, Y. El Amraoui, B. Marbati

Available online at www.sciencedirect.com

ScienceDirect

materialstoday: PROCEEDINGS

[ICP2020]

Effect of growth time on structural and surface properties of TiO_2 nanostructures deposited by single-step hydrothermal method

H. Mezzourh[a,b,*], S. Ben Moumen[a], M.Amjoud[a], D. Mezzane[a,b], Y. El Amraoui[c], B. Marbati[d], A.Lahmar[b], M. Jouiad[b], M. El Marssi[b]

[a] Laboratory of Innovative Materials, Energy and Sustainable Development (IMED), Cadi-Ayyad University, Faculty of Sciences and Technology, BP 549, Marrakech, Morocco.

[b] Laboratory of Physics of Condensed Matter (LPMC), University of Picardie Jules Verne, Scientific Pole, 33 rue Saint-Leu, 80039 Amiens Cedex 1, France.

[c] Laboratory of Condensed Matter and Interdisciplinary Sciences (LaMCScl), Faculty of Sciences, Mohammed V University of Rabat, P.O. Box 1014, Morocco.

[d] Center for Innovation and Technology Transfer (CITT), Moulay Ismail University, Meknes, Morocco.

Abstract

In this study, highly pure rutileTiO_2 nanorods (NRs) structures were grown on fluorine-doped tin oxide (FTO) coated glass substrates by using a one-step hydrothermal method. The effect of the growth time on the structure and surface properties of the obtained products has been studied. The X-ray diffraction analysis and the Raman spectroscopy indicated that the films were single-crystalline rutile phase. At lower hydrothermal time, TiO_2 NRs singly distributed with small diameter are found showing a high contact angle with ethylene glycol. When the hydrothermal reaction increases, nanoflowers (NFs) with a large diameter are formed over the TiO_2 NRs leading to superhydrophilic surfaces. These nanostructured thin films can be tailored to the requirements of specific applications involving water and ethylene glycol.

Keywords: TiO_2 nanorods/nanoflowers;hydrothermal; FTO/TiO_2; contact angle; superhydrophilicity; wettability.

* Corresponding author. Tel.: +212 670961694.

E-mail address: mezzourhhanane@gmail.com / hanane.mezzourh@ced.uca.ma

1. Introduction

Wettability and superhydrophilicity are some of the surface properties, which play an important role in a broad range of practical applications, including self-cleaning and anti-fogging, wear and erosion-resistant defensive, transportation of fluids in micro-fluidic devices, and development of bio-medical materials **[1]**. In general, surface wettability can be strongly controlled by surface chemistry, free energy, morphology, and liquid nature**[2]**. A facile way to express superwetting characteristics of a surface is by the contact angle (CA) of liquid droplets resting on the surface. Wettability studies require the measurement of contact angles as the primary data, which indicates the degree of wetting at the time of solid-liquid interaction**[3]**.

One-dimensional (1D) nanostructures (e.g., nanotubes, nanobelts, nanowires, nanorods, and nanoflowers) have been considered to be very attractive candidates for superhydrophilic (superwetting) surfaces fabrication due to their surface roughening**[4]**. Particularly, single-crystalline rutile TiO_2 nanostructures are considered to befavorable surface wettability materials because of their excellent chemical stability, structure controllability, specific interface effect, and low cost**[5]**. The superhydrophilic properties of TiO_2 nanostructures can be brought by many technologies, including plasma treatment, ultraviolet irradiation, laser treatment, ultrasonic spray pyrolysis, sol-gel process, anodization, electrospinning, laser deposition, microwave irradiation, and hydrothermal treatment **[1]**.

In this paper, we report a simple and fast growth of aligned TiO_2 nanostructures on FTO substrates by a one-step hydrothermal method. The influence of growth time on structure and surface properties was discussed.

2. Experimental procedure

2.1. Chemical and materials

All chemicals were used without any further treatment. Titanium (IV) isopropoxide (TTIP) with 98% purity was purchased from Sigma-Aldrich and used as a precursor. Hydrochloric acid (HCl) with 37% concentration was supplied by Labbox and used as a catalyst. Deionized (DI) water was obtained from local sources and FTO glass substrates from MSE Supplies.

2.2. Synthesis procedure

2.2.1. Substrate preparation

The substrates were ultrasonically cleaned in acetone, propan-2-ol, and absolute ethanolfor 30 min followed by deionized water. Then the substrates were dried under N_2 gas.

2.2.2. Preparation of aligned TiO_2 nanorods (NRs)

The synthesis of the TiO_2 nanorods (NRs)was performed by a single-step hydrothermal method under relatively acidic conditions on a transparent FTOcoated glass substrate. In a typical preparation, 10 mL of deionized water was mixed with 10 mL of concentrated hydrochloric acid solution to reach a total volume of 20 mL, and then the mixture was stirred for 10 min. A certain amount of titanium (IV) isopropoxide was added to the previous mixture solution to offer a sufficient titanium source and then stirred for 30 min. The final solution was transferred into a Teflon-lined stainlesssteel autoclave with a volume ratio of 2/3. Meanwhile, a clean piece of the FTO glass substrate was placed at the bottom of the autoclave. Then, the hydrothermal reaction was conducted at 180 °C for different reaction times at 1, 1.5, 2, and 3h. The corresponding samples are designated TO-x, where x is the growth time.

After the reaction time is over, the autoclave was cooled naturally to room temperature. The obtained samples were repeatedly rinsed with DI water and ethanol to remove impuritiesand finally dried with N_2 gas. Finally, the dried samples were annealed at 350 °C for 1h.

2.3. Technical characterization

Structural characterization of the prepared TiO_2 nanostructures was determined by X-ray diffraction (XRD, Panalytical X-Pert Pro) analysis using the Cu-Kα radiation with λ~1.540598 Å. The measurements were performed at a range angle from 20° to 80° with a step size of 0.02°. Morphological and compositional characterizationswere examined by a Scanning Electron Microscope (SEM, VEGA 3-Tscan) in association with energy dispersive X-ray (EDX) analysis. Contact angles were measured by defining a circle around the liquid drops (deionized water and ethylene glycol (EG) and recording the tangent angle formed at the substrate surface. The droplet volume used was 5μL.

3. Results and discussion

3.1. Structural analysis

Figure 1 shows XRD patterns for the FTO/TiO_2 nanostructures prepared at different reaction time intervals (1, 1.5, 2, and 3 hours) and the FTO substrate. All the diffraction peaks can be indexed as the tetragonal rutile structure of TiO_2 (JCPDS card number 89-4920). The diffraction peaks at 2θ of 26.88, 34.09, 38.11, 51.83, 61.89, and 65.79 are assigned to tin oxide (SnO_2) arising from FTO substrate (JCPDS card no. 41-1445). No impurity peaks have been detected from the XRD spectrums. By increasing the growth time, the peak intensities for the TiO_2 rutile phase increase at the expense of FTO peak intensities which could be explained by the increase in the thickness of the TiO_2 film. The diffraction pattern of TO-1h shows only one peak of rutile (211) at 2θ of 54.49°, while the film synthesized with a growth time of 1.5h reveals four peaks of rutile (101), (211), (002), and (301). The TO-2h and TO-3h show clearly peaks of the rutile phase, which is due to the fact that almost the entire surface of FTO has been completely covered with TiO_2 rutile-phased nanostructures. It should be noted that by increasing the growth time, the (002) peak gets more intense, suggesting that the degree of crystallinity and the crystallographic orientation growth along the [001] direction become more pronounced, resulting in the anisotropic growth of rutile TiO_2 nanorods along the [001] direction. The average crystallite size was estimated from XRD patterns using the Scherrer equation, and the found values are gathered in **Table 1**. It is observed that the average crystallite size of TiO_2nanostructures increases by increasing the growth time, indicating better crystallinity for a longer hydrothermal reaction time.

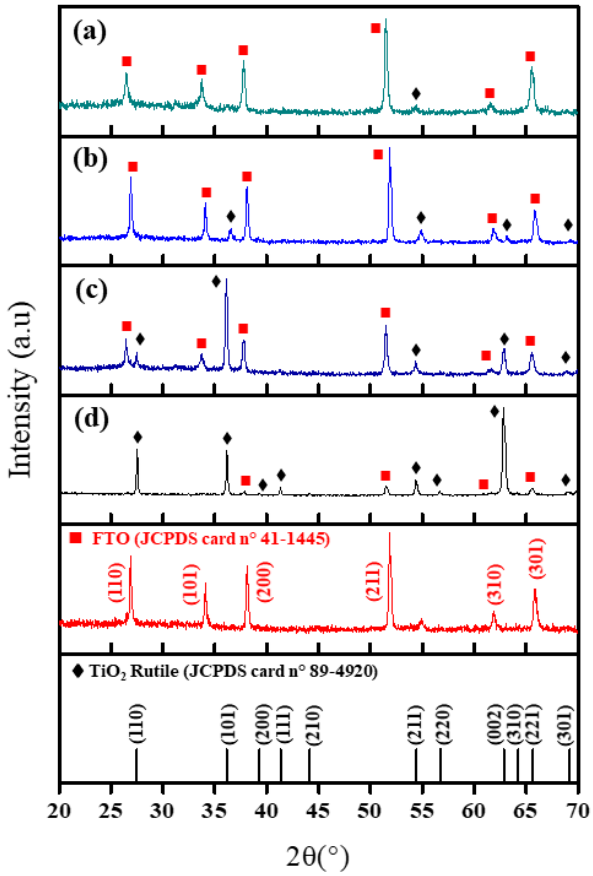

Fig.1. XRD patterns for TiO_2 nanostructures prepared via hydrothermal technique with different reaction times: (a) 1 h, (b) 1.5 h, (c) 2 h, and (d) 3 h.

Table.1. Average diameter size, FWHM, and average crystalline size of TiO_2 nanostructures prepared at different reaction times.

Reaction time (h)	Average diameter (nm) by SEM		FWHM	Average crystalline size (nm) by XRD
	NRs	NFs		
1	49.80	---	0.5510	16.22
1.5	114.06	111.86	0.3149	28.43
2	125.85	173.83	0.1574	56.76
3	250.35	582.08	0.0787	113.53

3.2. Raman spectroscopy

To evaluate the structural changes of the synthesized TiO_2 nanostructures, Raman spectroscopy was also performed. **Figure 2** shows the Raman spectra of TiO_2nanostructures at different reaction times (1, 1.5, 2, and 3h). The spectra reveal that no peaks other than those pertaining to rutile TiO_2 appear. It can be seen from the four spectra that the peak intensities are significantly increased with increasing the reaction time, which is in good accordance with the XRD results. After 3h of reaction, it is clearly seen that the first-order Raman scattering of rutile TiO_2 showed active fundamental modes at 149.0 cm^{-1} (B_{1g}), 234.9 cm^{-1}, 449.5 cm^{-1} (E_g), 613.3cm^{-1} (A_{1g}), and 826.5 cm^{-1} (B_{2g}). The two predominant maxima peaks located at 449.5 cm^{-1} and 613.3cm^{-1} correspond to the O–Ti–O bending vibrations and

Ti–O stretching vibrations of crystalline rutile TiO_2 phase, respectively **[6]**.Besides, there is a second-order scattering featured at about 234.9 cm^{-1} peak due to the multiple-phonon scattering process, which is also considered as a characteristic Raman peak of rutile TiO_2.

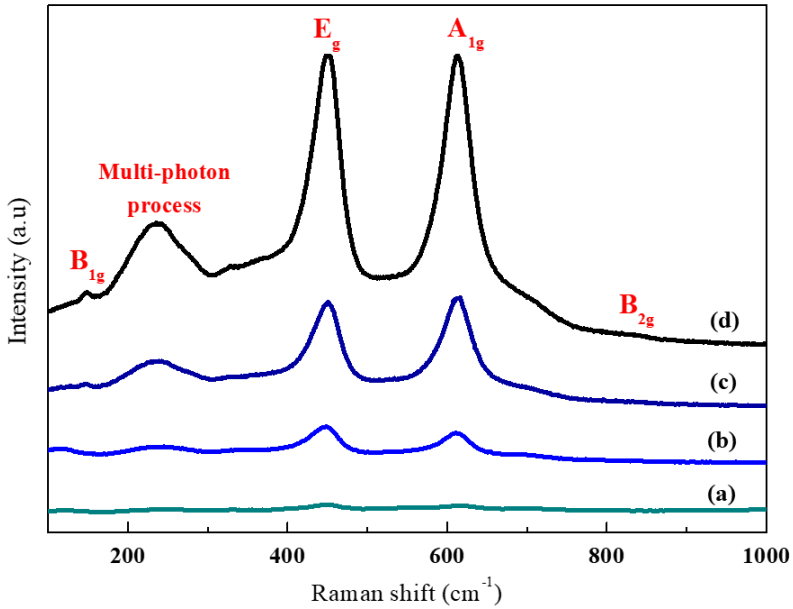

Fig.2. Raman spectra of samples (a) TO-1h, (b) TO-1.5h, (c) TO-2h, and (d) TO-3h.

3.3. Microstructure and compositional analyses

The surfaces' morphologies of the bare FTO substrate and FTO/TiO_2 nanostructures are observed and the results are shown in **Figure 3(a–f).** The SEM images revealed that the TiO_2 nanostructures with different densities, sizes, and shapes can be achieved by increasing the hydrothermal reaction time. At 1h of reaction time, the shapes of the structures were found to be nanorods singly distributed on FTO substrate with of diameter of about 50 nm **(Figure3b).** As the reaction time becomes longer, a significant increase in dimension of the resultant nanostructures is observed. The nanorods become larger and the gap between them decreases. Likewise, 3D nanoflowers (NFs) like arrangements of NRs are formed over the 1D nanorods as shown in **Figure3(b-e)**.As we can see in the zoom of the SEM micrograph in **Figure 3f**, the NRs developed on the TO-3h NRs surface reveal a regular tetragonal shape with smooth walls and square end, which is a signature of rutile crystal structure in accordance with XRD measurements **[7]**. Furthermore, the average size of NRs and NFs increases with increasing hydrothermal reaction time **(Table 1)**. It is apparent from this study that the hydrothermal reaction time has a significant effect on the TiO_2 NRs microstructure. Indeed, aligned TiO_2 NRs are found when the reaction time is less than 1.5h, but beyond this growth time, NFs become to grow over the NRs coating. According to the Wenzel theory**[8]**, these interesting roughness hierarchical TiO_2 NRs structure would be a benefit to enhance the wettability of surfaces. **Figure 4** shows the schematic illustration of the growth mechanism of TiO_2 nanorods on FTO substrate.

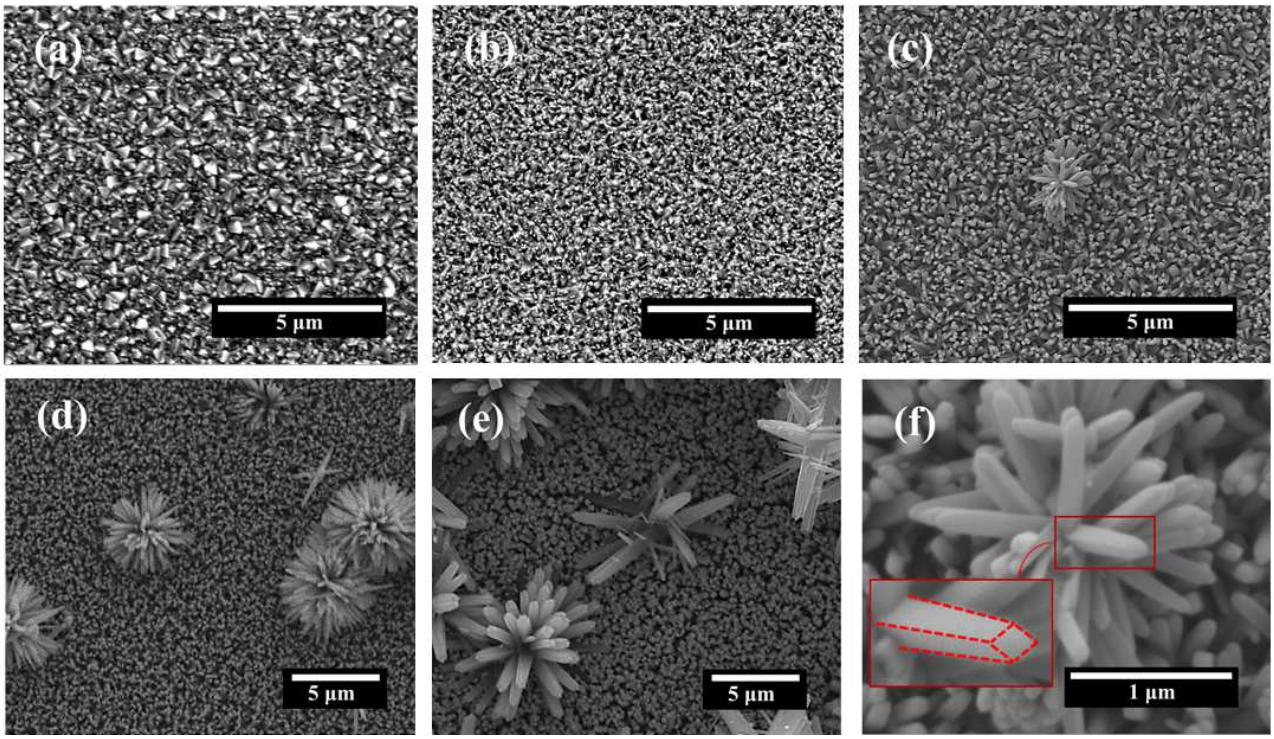

Fig.3. SEM images of a bare FTO substrate **(a)** and TiO_2 nanostructures prepared via hydrothermal technique with different reaction times: **(b)** 1 h, **(c)** 1.5 h, **(d)** 2 h, and **(e)** 3 h. (f) zoom of the NF growth on TO-1.5h NRs.

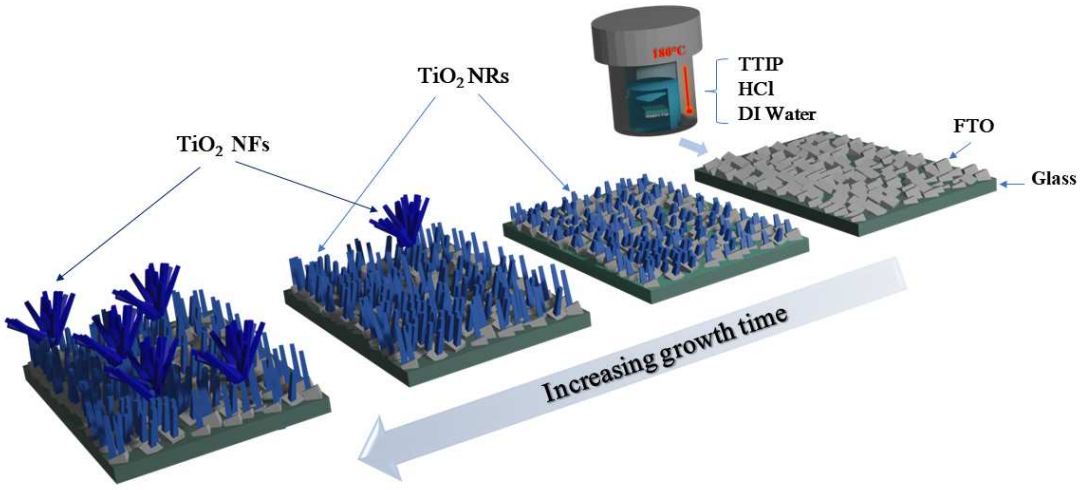

Fig.4. Scheme for growth mechanism of TiO_2 nanostructures on FTO substrate.

The elemental composition of theTO-1.5h sample was analyzed by EDX as shown in **Figure 5**, there is no trace of any other impurities that could be seen within the detection limit of the EDX. The corresponding EDX result indicates that the TO-1.5h film consists mainly of Ti and O with an approximate atomic ratio of 1:2 which is in consistent with the stoichiometry of TiO_2. Hence, EDX analysis confirms the formation of TiO_2.

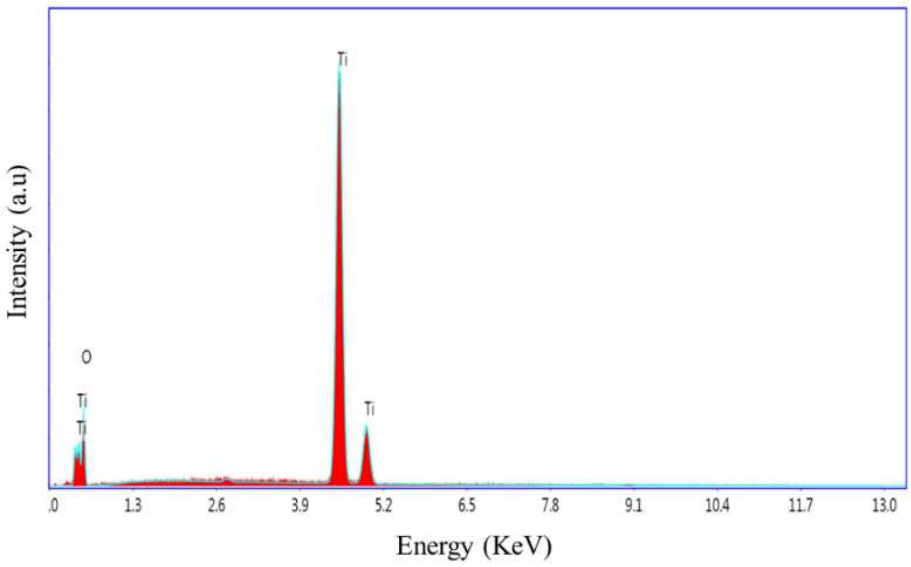

Fig.5. EDX spectrum of TiO_2 nanostructures prepared at 1.5 h reaction time.

3.4. Wetting properties

The interfacial reaction of TiO_2 nanostructures could be followed by measuring the contact angle. According to the Young's equation **[9],**the contact angle θ of a droplet on the surface can be described as:

$$Cos\ \theta_e = \frac{\gamma_{SV} - \gamma_{SL}}{\gamma_{LV}} \qquad (1)$$

Where θ_e is the equilibrium contact angle. γ_{SV}, γ_{SL}, and γ_{LV}, are the interface energies at the solid-vapor, solid-liquid, and liquid-vapor interfaces, respectively.

Depending on the contact angle obtained, we can define the characteristics of the observed surfaces. If the resulting contact angle is 0°, the surface is mentioned as superhydrophilic and if it is less than 90°, the surface is hydrophilic. If the CA is between 90 and 180°, the surface is hydrophobic and if the angle is greater than 180°, the surface is superhydrophobic.

It should be noted that the wetting behavior of a solid surface depends not only on the properties of the liquid and the chemical properties of the solid surface but also on its roughness. Thus, to create superhydrophilicity, the surface roughness must be controlled to maximize the contact area and interaction between liquid and the solid surface.Wenzel and Cassie-Baxter suggested two models to describe the wetting phenomena on rough surfaces. According to Wenzel's model, the water droplet seeps in between the irregularities of a rough surface increasing the contact area between the solid surface and the liquid. On the other hand, for the Cassie–Baxter model, the water droplet sits on top of the surface structure without much penetration[10], [11]. The rougher the surface, the higher will be the contact angle.

To investigate the wettability property of the TiO_2 nanostructures, the water and ethylene glycol contact angle measurements were carried out. **Figure 6** shows the change in the contact angle of TiO_2 nanostructures at various growth times. The TiO_2 surfaces were completely wetted by water and exhibited almost zero water contact angles (WCA).This superhydrophilicity could be attributed to the rough TiO_2 NRs surface and to the presence of hydroxyl groups on its surfaces[12]. Because of the capillary effects of the rough surface, the water droplet can be induced to

enter into the NRs and fill the grooves of the coating according to the model proposed by Wenzel **[8]**. The TiO_2 nanostructures show a good wetting surfaces compared with other TiO_2 films reported in the literature (see **Table 2**). Furthermore, these nanostructures present a perfect wetting similar to that reported by W. Yang et al. and R. Dong.

In the case of ethylene glycol (EG), widely used as coolant and antifreeze agent in many commercial and industrial applications [13] the as-prepared TiO_2 nanostructures at 1h have produced a large contact angle of 83.3°. It is important to highlight that higher CA of ethylene glycol is very useful for its application as a corrosion inhibitor in cleaning processes [13]. When the growth time increases, the EG contact angle decreases abruptly to a very small value of CA about 5° for TO-3h, showing a good surface wettability. This trend can be explained by the formation of a highly porous TiO_2 structure to increase the surface roughness to achieve superhydrophilic surfaces as it has been noted by several authors [14], [15].

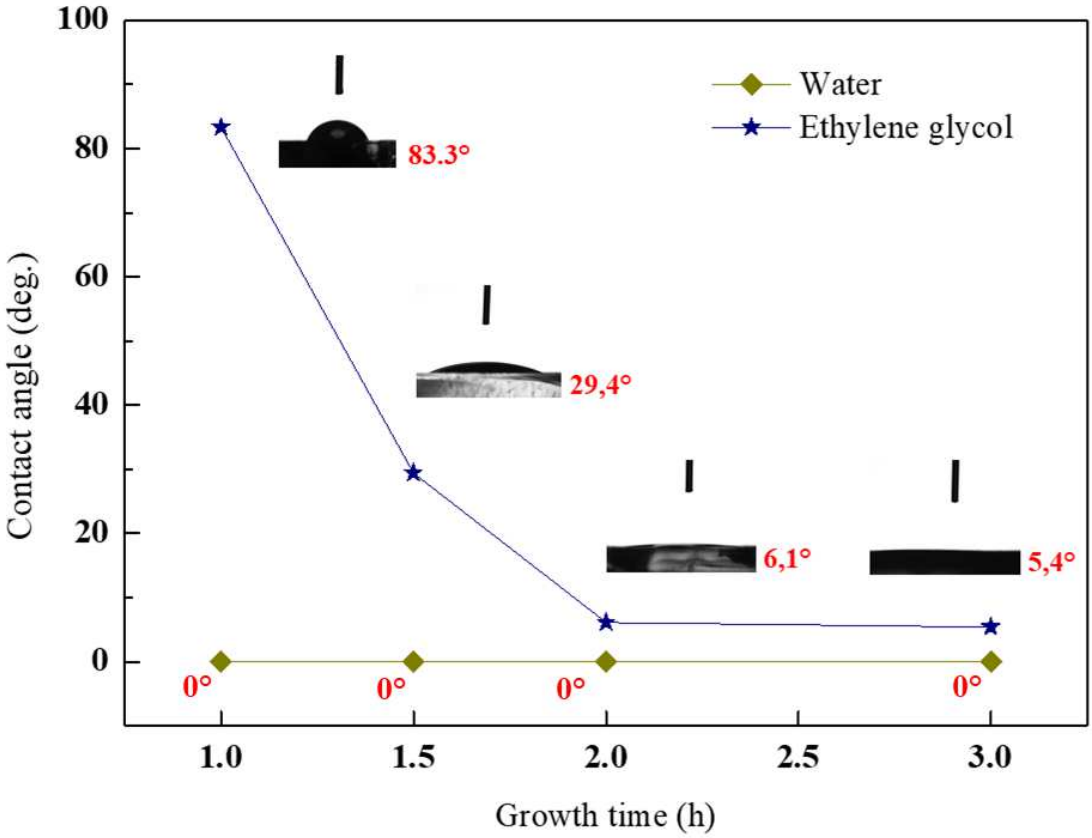

Fig.6. Contact angle properties of TiO_2 nanostructures at different growth times.

Table.2. Comparison of the contact angle properties of TiO_2 nanostructures prepared at different reaction times with other TiO_2 films reported in the literature.

Sample	Morphology	Diameter (nm)	Solvent	Contact angle (°)	Illuminating source	Surface wettability	Refs
TO-1h nanostructured film	Nanorods Nanoflowres	49.80	Water	0	Visible light	Perfect wetting	Our work
			Ethylene glycol	83.3	Visible light	High wetting	
TO-1.5h nanostructured film	Nanorods Nanoflowres	114.06	Water	0	Visible light	Perfect wetting	Our work
			Ethylene glycol	29.4	Visible light	High wetting	
TO-2h nanostructured film	Nanorods Nanoflowres	125.85	Water	0	Visible light	Perfect wetting	Our work
			Ethylene glycol	6.1	Visible light	High wetting	
TO-3h nanostructured film	Nanorods Nanoflowres	250.35	Water	0	Visible light	Perfect wetting	Our work
			Ethylene glycol	5.4	Visible light	High wetting	
TiO_2 nanotube arrays	Nanotubes	Not specified	Water	0	UV illumination	Perfect wetting	[16]
TiO_2 nanorod film	Nanorods	250	Water	0	Visible light	Perfect wetting	[17]
TiO_2 nanosheet array films	Nanosheets	30-70	Water	3	UV illumination	High wetting	[18]
TiO_2 film	Nanoparticles	100–200	Water	< 10	Visible light	High wetting	[19]
TiO_2 film	Nanoparticles	50	Water	≈ 30	UV illumination	High wetting	[20]
TiO_2 nanorods	Nanorods	97 - 120	Water	31 - 37	Not specified	High wetting	[21]

4. Conclusion

Superhydrophilic rutile TiO_2 Nanorod Arrays surfaces covered with NFs-like structure have been successfully fabricated on the FTO coated glass deposited by a single-step hydrothermal method. The CA on the as-deposited surfaces can reach 0° for water and 5° for EG droplets, showing outstanding superhydrophilicity. The formation of more nanoflowers with a large diameter on the top of the nanorods layer improves the surface wettability; whereas nanostructured film with smaller nanorods formed at a low hydrothermal time produced a higher contact angle of 83° with EG. These findings are of crucial interest for the design of self-cleaning surfaces and erosion-resistant defensive.

ACKNOWLEDGMENTS:

This research was supported by CNRST Priority Program PPR 15/2015 and the European H2020-MSCA-RISE-2017-ENGIMA action.

References

[1] T. A. Otitoju, A. L. Ahmad, et B. S. Ooi, « Superhydrophilic (superwetting) surfaces: A review on fabrication and application », *Journal of Industrial and Engineering Chemistry*, vol. 47, p. 19-40, mars 2017, doi: 10.1016/j.jiec.2016.12.016.

[2] I. Badge, A. Y. Stark, E. L. Paoloni, P. H. Niewiarowski, et A. Dhinojwala, « The Role of Surface Chemistry in Adhesion and Wetting of Gecko Toe Pads », *Sci Rep*, vol. 4, nº 1, p. 6643, mai 2015, doi: 10.1038/srep06643.

[3] T. Koishi, K. Yasuoka, S. Fujikawa, et X. C. Zeng, « Measurement of Contact-Angle Hysteresis for Droplets on Nanopillared Surface and in the Cassie and Wenzel States: A Molecular Dynamics Simulation Study », *ACS Nano*, vol. 5, nº 9, p. 6834-6842, sept. 2011, doi: 10.1021/nn2005393.

[4] R. W. Jaggers, R. Chen, et S. A. F. Bon, « Control of vesicle membrane permeability with catalytic particles », *Mater. Horiz.*, vol. 3, nº 1, p. 41-46, 2016, doi: 10.1039/C5MH00093A.
[5] M. Lv *et al.*, « Densely aligned rutile TiO_2 nanorod arrays with high surface area for efficient dye-sensitized solar cells », *Nanoscale*, vol. 4, nº 19, p. 5872, 2012, doi: 10.1039/c2nr31431b.
[6] C. Garapon *et al.*, « Preparation of TiO_2 thin films by pulsed laser deposition for waveguiding applications », *Applied Surface Science*, vol. 96-98, p. 836-841, avr. 1996, doi: 10.1016/0169-4332(95)00593-5.
[7] B. Fu, Z. Wu, S. Cao, K. Guo, et L. Piao, « Effect of aspect ratios of rutile TiO_2 nanorods on overall photocatalytic water splitting performance », *Nanoscale*, vol. 12, nº 8, p. 4895-4902, 2020, doi: 10.1039/C9NR10870J.
[8] R. N. Wenzel, « RESISTANCE OF SOLID SURFACES TO WETTING BY WATER », *Ind. Eng. Chem.*, vol. 28, nº 8, p. 988-994, août 1936, doi: 10.1021/ie50320a024.
[9] D. H. Shin, T. Shokuhfar, C. K. Choi, S.-H. Lee, et C. Friedrich, « Wettability changes of TiO_2 nanotube surfaces », *Nanotechnology*, vol. 22, nº 31, p. 315704, août 2011, doi: 10.1088/0957-4484/22/31/315704.
[10] Arshad, G. Momen, M. Farzaneh, et A. Nekahi, « Properties and applications of superhydrophobic coatings in high voltage outdoor insulation: A review », *IEEE Trans. Dielect. Electr. Insul.*, vol. 24, nº 6, p. 3630-3646, déc. 2017, doi: 10.1109/TDEI.2017.006725.
[11] Y. Cho et C. H. Park, « Objective quantification of surface roughness parameters affecting superhydrophobicity », *RSC Adv.*, vol. 10, nº 52, p. 31251-31260, 2020, doi: 10.1039/D0RA03137B.
[12] M.-K. Lee et Y.-C. Park, « Contact Angle Relaxation and Long-Lasting Hydrophilicity of Sputtered Anatase TiO_2 Thin Films by Novel Quantitative XPS Analysis », *Langmuir*, vol. 35, nº 6, p. 2066-2077, févr. 2019, doi: 10.1021/acs.langmuir.8b03258.
[13] K. H. Patel et S. K. Rawal, « Contact angle hysteresis, wettability and optical studies of sputtered zinc oxide nanostructured thin films », *INDIAN J. ENG. MATER. SCI.*, p. 8, 2017.
[14] H. Y. Lee, Y. H. Park, et K. H. Ko, « Correlation between Surface Morphology and Hydrophilic/Hydrophobic Conversion of MOCVD−TiO_2 Films », *Langmuir*, vol. 16, nº 18, p. 7289-7293, sept. 2000, doi: 10.1021/la9915567.
[15] J.-J. Wang, D.-S. Wang, J. Wang, W.-L. Zhao, et C.-W. Wang, « High transmittance and superhydrophilicity of porous TiO_2/SiO_2 bi-layer films without UV irradiation », *Surface and Coatings Technology*, vol. 205, nº 12, p. 3596-3599, mars 2011, doi: 10.1016/j.surfcoat.2010.12.033.
[16] W. Yang, Q. Peng, R. Chen, Y. Wen, et B. Shan, « Correlation between Hydrophilicity and Surface Aggregation in Anodized TiO_2 Nanotube Arrays », *Physics Procedia*, vol. 48, p. 220-227, 2013, doi: 10.1016/j.phpro.2013.07.035.
[17] R. Dong, S. Jiang, Z. Li, Z. Chen, H. Zhang, et C. Jin, « Superhydrophilic TiO_2 nanorod films with variable morphology grown on different substrates », *Materials Letters*, vol. 152, p. 151-154, août 2015, doi: 10.1016/j.matlet.2015.03.100.
[18] L. Lai *et al.*, « A facile hydrothermal synthesis and properties of TiO_2 nanosheet array films », *Mater. Res. Express*, vol. 7, nº 1, p. 015053, janv. 2020, doi: 10.1088/2053-1591/ab638b.
[19] Y. Kameya et H. Yabe, « Optical and Superhydrophilic Characteristics of TiO_2 Coating with Subwavelength Surface Structure Consisting of Spherical Nanoparticle Aggregates », *Coatings*, vol. 9, nº 9, p. 547, août 2019, doi: 10.3390/coatings9090547.
[20] X. Kong, Y. Hu, X. Wang, et W. Pan, « Effect of surface morphology on wettability conversion », *J Adv Ceram*, vol. 5, nº 4, p. 284-290, déc. 2016, doi: 10.1007/s40145-016-0201-5.
[21] T. Plirdpring *et al.*, « Preparation and surface wettability of nanostructure TiO_2 films », *Materials Today: Proceedings*, vol. 4, nº 5, p. 6331-6335, 2017, doi: 10.1016/j.matpr.2017.06.135.